Distribution of Inner Product of Complex Gaussian Random Vectors and its Applications

Ranjan K. Mallik, *Senior Member, IEEE,* and Nikos C. Sagias, *Member, IEEE*

***Abstract*—Let X and Y be two independent $L \times 1$ complex Gaussian random vectors distributed as $\mathcal{CN}(\mathbf{m}_X, \sigma_X^2 \mathbf{I}_L)$ and $\mathcal{CN}(\mathbf{m}_Y, \sigma_Y^2 \mathbf{I}_L)$, respectively, where $\mathbf{I}_L$ denotes the $L \times L$ identity matrix. The joint characteristic function (c.f.) of the real and imaginary parts of the inner product $\mathbf{Y}^H \mathbf{X}$ is derived in closed form, with $(\cdot)^H$ denoting the conjugate transpose. Based on this joint c.f., a unified analytical framework for the derivation of the average symbol error probability (ASEP) of a multibranch diversity reception system over flat correlated fading using M-ary phase-shift keying is developed. The receiver employs maximal-ratio combining with least squares channel estimation by means of pilot symbols. The optimal average pilot-to-noise power ratio is obtained in closed form, and the analytical framework is applied to Nakagami and Rice fading. For Nakagami fading, closed form ASEP expressions are obtained for the cases of high signal-to-noise (SNR) and binary phase-shift keying, while for Rice fading, high SNR approximate expressions are obtained in terms of a single integral under the constant correlation model and for independent and identically distributed channels. Both analytical and computer simulation results are presented and compared in order to verify the validity of the proposed analysis.**

***Index Terms*—Complex Gaussian vectors, imperfect channel estimation, inner product, least squares estimation, M-ary phase-shift keying (MPSK), maximal-ratio combining (MRC), pilot symbols, symbol error probability (SEP).**

I. Introduction

WIRELESS communication systems using multibranch diversity reception often employ maximal-ratio combining (MRC) at the receiver, since this scheme maximizes the instantaneous signal-to-noise ratio (SNR), and consequently, gives the best performance among various linear combining schemes. The MRC scheme, however, needs channel estimates. In practice, these estimates are imperfect since they are perturbed by additive noise resulting from the channel estimation method used, and this causes the system performance to degrade. It is therefore important that we study the effect of such imperfections in the channel state information (CSI) and tune the system parameters to compensate for the degradation.

Paper approved by A. Zanella, the Editor for Wireless Systems of the IEEE Communications Society. Manuscript received January 18, 2011; revised June 6, 2011 and August 21, 2011.

This paper was presented in part at the IEEE International Conference on Communications, Beijing, China, May 2008.

The work of R. K. Mallik was supported in part by the IDRC Research Grant RP02253.

R. K. Mallik is with the Department of Electrical Engineering, Indian Institute of Technology—Delhi, Hauz Khas, New Delhi 110016, India (e-mail: rkmallik@ee.iitd.ernet.in).

N. C. Sagias is with the Department of Telecommunications Science and Technology, School of Applied Sciences and Technology, University of Peloponnese, end of Karaiskaki Street, 22100, Tripoli, Greece (e-mail: nsagias@ieee.org).

Digital Object Identifier 10.1109/TCOMM.2011.101011.110046

The error performance for MRC systems with M-ary phase-shift keying (MPSK) and imperfect channel estimation has been studied in [1] in case of independent branches, assuming Rayleigh or Rice fading, and an error probability expression in the form of a higher order derivative has been obtained. The distribution of the phase angle of two deterministic vectors perturbed by Gaussian noise, which can be applied to MPSK performance analysis, has been derived in [2] and [3] using different approaches. The case of binary phase-shift keying (BPSK) with MRC and different fading conditions has been analyzed in [4], resulting in integral expressions for the error probability. The effect of imperfect channel estimation on the error performance of MPSK with MRC in generalized Rice fading channel has been studied in [5]. The analysis considers various channel estimation methods, with all results being in the form of an inverse Laplace transform that can be computed using analytical techniques. In [6], optimal combining has been studied for BPSK modulation over correlated Rayleigh fading with minimum mean square error (MMSE) channel estimation and the average bit error probability (ABEP) has been obtained in analytical form. A later contribution [7] has extended [6] to Rice fading with the results being in terms of a single integral, while the optimal pilot power allocation has been also investigated.

It is to be noted that the error performance of MPSK with MRC using imperfect channel estimates can be analyzed directly from the distribution of the inner product of two complex Gaussian vectors. Motivated by this, we first derive the joint characteristic function (c.f.) of the real and imaginary parts of the inner product of two independent complex Gaussian vectors having arbitrary mean vectors and covariance matrices, which are scaled versions of the identity matrix. This joint c.f. is then used to develop a unified analytical framework for the analysis of the average symbol error probability (ASEP) of multibranch diversity reception systems operating over flat correlated fading using MPSK. The receiver employs MRC with least squares channel estimation by means of pilot symbols. The usefulness of the analytical framework is demonstrated by its application to Nakagami and Rice fading scenarios. For Nakagami fading, closed form ASEP expressions are obtained for the cases of high SNR and BPSK, while for Rice fading simple approximate expressions in terms of a single integral are obtained under the constant correlation model and for independent and identically distributed (i.i.d.) channels. In addition, the optimal average pilot-to-noise ratio (PNR) is obtained in closed form.

The paper is organized as follows. Section II provides a theorem concerning the joint c.f. of the real and imaginary

$$\Psi_{Z_1,Z_2}(\jmath\omega_1,\jmath\omega_2) = \frac{1}{\left(1+\frac{\left(\omega_1^2+\omega_2^2\right)}{4}\sigma_X^2\,\sigma_Y^2\right)^L} \times \exp\left\{-\frac{\frac{\left(\omega_1^2+\omega_2^2\right)}{4}\left(\|\mathbf{m}_X\|^2\sigma_Y^2+\|\mathbf{m}_Y\|^2\sigma_X^2\right)-\jmath\omega_1\,\Re\left(\mathbf{m}_Y^H\,\mathbf{m}_X\right)-\jmath\omega_2\,\Im\left(\mathbf{m}_Y^H\,\mathbf{m}_X\right)}{1+\frac{\left(\omega_1^2+\omega_2^2\right)}{4}\sigma_X^2\,\sigma_Y^2}\right\} \tag{2}$$

parts of the inner product of two complex Gaussian vectors. In Section III, the system model under consideration is presented. The analytical framework of Sections II and III is used in Section IV to derive unified ASEP expressions for BPSK, quadriphase-shift keying (QPSK), and MPSK. Section V studies the optimal pilot power allocation issue. Specific ASEP expressions for Rayleigh, Rice, and Nakagami fading are presented in Section VI, while numerical and computer simulation results are demonstrated in Section VII. Concluding remarks are given in Section VIII.

II. Statistic of the Inner Product of Two Complex Gaussian Random Vectors

Theorem 1 (Inner Product Joint C.F. of Random Vectors): Let $\mathbf{X} = [X_1\, X_2 \cdots X_L]^T$ and $\mathbf{Y} = [Y_1\, Y_2 \cdots Y_L]^T$, where $(\cdot)^T$ denotes the transpose operator, be two independent complex Gaussian vectors distributed as $\mathcal{CN}(\mathbf{m}_X, \sigma_X^2\,\mathbf{I}_L)$ and $\mathcal{CN}(\mathbf{m}_Y, \sigma_Y^2\,\mathbf{I}_L)$, respectively, where $\mathbf{I}_L$ denotes the $L \times L$ identity matrix, $\mathbf{m}_X = \mathbf{E}[\mathbf{X}]$, $\mathbf{m}_Y = \mathbf{E}[\mathbf{Y}]$, and $\sigma_X^2 = \mathbf{E}[|X_i|^2] - \mathbf{E}^2[|X_i|]$, $\sigma_Y^2 = \mathbf{E}[|Y_i|^2] - \mathbf{E}^2[|Y_i|]$ $\forall i = 1, 2, \ldots, L$, with $\mathbf{E}[\cdot]$ denoting the expectation operator. Let the inner product of $\mathbf{X}$ and $\mathbf{Y}$ be given by the complex random variable Z, such that

$$Z = \mathbf{Y}^H\,\mathbf{X}, \tag{1}$$

where $(\cdot)^H$ is the Hermitian (conjugate transpose) operator, and also let $Z_1 = \Re(Z)$ and $Z_2 = \Im(Z)$ denote the real and imaginary parts of Z, respectively. Then, the joint c.f. of Z_1 and Z_2 is given by (2), as shown on the top of this page, where $\jmath = \sqrt{-1}$ and $\|\cdot\|$ denotes the Euclidean norm.

Proof: From (1) and the distribution of $\mathbf{X}$, it is clear that Z_1 and Z_2, conditioned on $\mathbf{Y}$, are independent, and their conditional distributions are given by

$$Z_1|_{\mathbf{Y}} \sim \mathcal{N}\left(\Re\left(\mathbf{Y}^H\mathbf{m}_X\right),\ \frac{\sigma_X^2}{2}\|\mathbf{Y}\|^2\right), \tag{3a}$$

$$Z_2|_{\mathbf{Y}} \sim \mathcal{N}\left(\Im\left(\mathbf{Y}^H\mathbf{m}_X\right),\ \frac{\sigma_X^2}{2}\|\mathbf{Y}\|^2\right), \tag{3b}$$

where "$\sim$" stands for "is distributed as." The conditional joint c.f. of Z_1 and Z_2, conditioned on $\mathbf{Y}$, is therefore expressed as

$$\Psi_{Z_1,Z_2|\mathbf{Y}}(\jmath\omega_1,\jmath\omega_2|\mathbf{y}) = \mathbf{E}\left[\exp\left\{\jmath\left(\omega_1 Z_1+\omega_2 Z_2\right)\right\}\middle|\,\mathbf{Y}=\mathbf{y}\right] = \exp\left\{\jmath\left(\omega_1\,\Re\left(\mathbf{y}^H\mathbf{m}_X\right)+\omega_2\,\Im\left(\mathbf{y}^H\mathbf{m}_X\right)\right) -\frac{1}{4}\left(\omega_1^2+\omega_2^2\right)\sigma_X^2\|\mathbf{y}\|^2\right\}. \tag{4}$$

The probability density function (p.d.f.) of $\mathbf{Y}$ is given by

$$f_{\mathbf{Y}}(\mathbf{y}) = \frac{1}{\pi^L\,\sigma_Y^{2L}}\exp\left\{-\frac{\|\mathbf{y}-\mathbf{m}_Y\|^2}{\sigma_Y^2}\right\}, \quad \mathbf{y}\in\mathcal{C}^L, \tag{5}$$

where $\mathcal{C}$ denotes the set of complex numbers. The joint c.f. of Z_1 and Z_2 can now be expressed in terms of the p.d.f. of $\mathbf{Y}$ as

$$\Psi_{Z_1,Z_2}(\jmath\omega_1,\jmath\omega_2) = \mathbf{E}\left[\exp\left\{\jmath\left(\omega_1 Z_1+\omega_2 Z_2\right)\right\}\right] = \int_{\mathbf{y}\in\mathcal{C}^L}\Psi_{Z_1,Z_2|\mathbf{Y}}(\jmath\omega_1,\jmath\omega_2|\mathbf{y})f_{\mathbf{Y}}(\mathbf{y})d\mathbf{y}. \tag{6}$$

Substituting (4) and (5) in (6), we get

$$\Psi_{Z_1,Z_2}(\jmath\omega_1,\jmath\omega_2) = \frac{\exp\left\{-\|\mathbf{m}_Y\|^2/\sigma_Y^2\right\}}{\pi^L\sigma_Y^{2L}} \times\int_{\mathbf{y}\in\mathcal{C}^L}\exp\left\{-\left(\frac{1}{\sigma_Y^2}+\frac{\left(\omega_1^2+\omega_2^2\right)}{4}\sigma_X^2\right)\|\mathbf{y}\|^2 + 2\,\Re\left(\mathbf{y}^H\left(\frac{1}{\sigma_Y^2}\mathbf{m}_Y\right)\right)+\jmath\,2\,\Re\left(\mathbf{y}^H\left(\frac{(\omega_1-\jmath\omega_2)}{2}\mathbf{m}_X\right)\right)\right\}d\mathbf{y}. \tag{7}$$

Note that [2], [8]

$$\frac{1}{\pi^L}\int_{\mathbf{y}\in\mathcal{C}^L}\exp\left\{-a\|\mathbf{y}\|^2+2\,\Re\left(\mathbf{y}^H\mathbf{b}\right)+\jmath\,2\,\Re\left(\mathbf{y}^H\mathbf{c}\right)\right\}d\mathbf{y} = \frac{1}{a^L}\exp\left\{\frac{\|\mathbf{b}\|^2-\|\mathbf{c}\|^2+\jmath\,2\,\Re\left(\mathbf{b}^H\mathbf{c}\right)}{a}\right\}, \tag{8}$$

with $a > 0$, $\mathbf{b}, \mathbf{c} \in \mathcal{C}^L$. Applying the result (8) in (7), we obtain (9), as shown on the top of the next page. Simplification of (9) yields (2). ■

III. Multibranch Diversity Reception

We now present the required analytical framework concerning the system model, including the channel estimation method and decision statistics. Consider a diversity reception system having L branches in a flat fading environment using MPSK with symbol-by-symbol detection. The $L\times 1$ sampled complex baseband signal vector received over the L diversity branches in a symbol interval can be expressed as

$$\mathbf{r} = s\,\mathbf{h} + \mathbf{n}, \tag{10}$$

where s is the information-bearing signal (or symbol) that belongs to an MPSK constellation S, given by

$$S = \{S_1, S_2, \ldots, S_M\}, \tag{11}$$

$$\Psi_{Z_1,Z_2}(\jmath\omega_1,\jmath\omega_2)=\frac{\exp\left\{-\frac{\|\mathbf{m}_Y\|^2}{\sigma_Y^2}\right\}}{\sigma_Y^{2L}\left(\frac{1}{\sigma_Y^2}+\frac{\left(\omega_1^2+\omega_2^2\right)}{4}\sigma_X^2\right)^L}\exp\left\{\frac{\frac{\|\mathbf{m}_Y\|^2}{\sigma_Y^4}-\frac{\left(\omega_1^2+\omega_2^2\right)}{4}\|\mathbf{m}_X\|^2+\jmath\frac{1}{\sigma_Y^2}\Re\left((\omega_1-\jmath\omega_2)\,\mathbf{m}_Y^H\,\mathbf{m}_X\right)}{\frac{1}{\sigma_Y^2}+\frac{\left(\omega_1^2+\omega_2^2\right)}{4}\sigma_X^2}\right\} \quad (9)$$

where

$$S_\ell=\sqrt{2\,E_s}\,\exp\left\{\jmath\,2\,\pi\,\frac{(\ell-1)}{M}\right\},\quad \ell=1,2,\ldots,M, \quad (12)$$

with $2E_s$ denoting the average symbol energy, $\mathbf{h}$ is the complex random channel gain vector and $\mathbf{n}$ is the additive white Gaussian noise (AWGN) vector, which is a zero-mean complex circular Gaussian vector with covariance matrix $2N_0\mathbf{I}_L$ and is independent of $\mathbf{h}$. Thus, $\mathbf{n}$ has a $\mathcal{CN}(\mathbf{0}_L, 2N_0\mathbf{I}_L)$ distribution, where $\mathbf{0}_L$ denotes the $L\times 1$ vector of zeros.

A. Least Squares Channel Estimation

The CSI $\mathbf{h}$ is estimated by transmitting a sequence $s_{p_1}, s_{p_2}, \ldots, s_{p_K}$ of K pilot symbols (which are known to the receiver) prior to data transmission (transmission of s in (10)). The received signal vector corresponding to the kth pilot symbol transmission can be expressed as

$$\mathbf{r}_{p_k}=\mathbf{h}s_{p_k}+\mathbf{n}_{p_k}\,,\quad k=1,\ldots,K, \quad (13)$$

where $\mathbf{n}_{p_k}$ is the kth pilot AWGN vector (independent of $\mathbf{h}$). The pilot noise vectors $\mathbf{n}_{p_1}, \mathbf{n}_{p_2}, \ldots, \mathbf{n}_{p_K}$ are i.i.d. complex circular Gaussian vectors, each having a $\mathcal{CN}(\mathbf{0}_L, 2N_0\mathbf{I}_L)$ distribution, and are independent of $\mathbf{n}$.

Let $\mathbf{s}_p=[s_{p_1}\,s_{p_2}\cdots s_{p_K}]^T$ be the pilot symbol vector. If $\mathbf{r}_p$ and $\mathbf{n}_p$ represent the concatenated received signal vector over K pilot transmissions and the concatenated pilot AWGN vector, respectively, given by

$$\mathbf{r}_p=[\mathbf{r}_{p_1}\,\mathbf{r}_{p_2}\cdots\mathbf{r}_{p_K}]^T\,,\quad \mathbf{n}_p=[\mathbf{n}_{p_1}\,\mathbf{n}_{p_2}\cdots\mathbf{n}_{p_K}]^T\,, \quad (14)$$

then (13) can be rewritten as

$$\mathbf{r}_p=(\mathbf{s}_p\otimes\mathbf{I}_L)\,\mathbf{h}+\mathbf{n}_p\,, \quad (15)$$

where $\otimes$ denotes the Kronecker product of matrices.

We obtain the CSI $\mathbf{h}$ from $\mathbf{r}_p$ using least squares estimate (LSE). From (15), the LSE $\hat{\mathbf{h}}$ of the channel gain vector can be expressed as

$$\hat{\mathbf{h}}=\frac{1}{\|\mathbf{s}_p\|^2}\left(\mathbf{s}_p^H\otimes\mathbf{I}_L\right)\mathbf{r}_p\,. \quad (16)$$

Substituting (15) in (16), the LSE of $\mathbf{h}$ is given by

$$\hat{\mathbf{h}}=\mathbf{h}+\mathbf{v}\,, \quad (17)$$

where

$$\mathbf{v}=\frac{1}{\|\mathbf{s}_p\|^2}\left(\mathbf{s}_p^H\otimes\mathbf{I}_L\right)\mathbf{n}_p \quad (18)$$

is independent of $\mathbf{h}$ and

$$\mathbf{v}\sim\mathcal{CN}\left(\mathbf{0}_L,\frac{2N_0}{\|\mathbf{s}_p\|^2}\mathbf{I}_L\right).$$

B. Detection Rule

The reception of K pilot symbols is followed by the symbol-by-symbol reception and detection of data. For a transmitted data symbol s in a symbol interval, the signals received over the L diversity branches (given by vector $\mathbf{r}$ in (10)) are combined using MRC by means of the LSE $\hat{\mathbf{h}}$ of the channel, resulting in the *combiner output* $\hat{\mathbf{h}}^H\mathbf{r}$. From this output, the detected symbol $\hat{s}$ is obtained using the decision rule

$$\hat{s}=\arg\left\{\max_{s\in S}\,\Re\left(s^*\,\hat{\mathbf{h}}^H\,\mathbf{r}\right)\right\}, \quad (19)$$

where $(\cdot)^*$ denotes the complex conjugate.

IV. Symbol Error Probability Analysis of MPSK

From the analytical framework of Sections II and III, this section presents a unified framework for the ASEP performance of MPSK employing MRC and LSE. When the symbol S_ℓ (given by (12)) is transmitted, the combiner output can be expressed using (10) and (17) as

$$\begin{aligned}\hat{\mathbf{h}}^H\mathbf{r}\Big|_{s=S_\ell}&=(\mathbf{h}+\mathbf{v})^H\,(\mathbf{h}\,S_\ell+\mathbf{n})\\&=\sqrt{2\,E_s}\,\exp\left\{\jmath\,\frac{2\,\pi\,(\ell-1)}{M}\right\}(\mathbf{h}+\mathbf{v})^H\,(\mathbf{h}+\mathbf{u})\,,\end{aligned} \quad (20)$$

where

$$\mathbf{u}=\frac{1}{\sqrt{2\,E_s}}\,\exp\left\{-\jmath\,\frac{2\,\pi\,(\ell-1)}{M}\right\}\mathbf{n} \quad (21)$$

and has a $\mathcal{CN}(\mathbf{0}_L,(N_0/E_s)\,\mathbf{I}_L)$ distribution which is independent of $\mathbf{v}$.

Let Γ denote the *average SNR per branch and per symbol*, and Γ_p the *average PNR per symbol*, defined as

$$\Gamma\triangleq\frac{E_s}{N_0} \quad (22a)$$

and

$$\Gamma_p\triangleq\frac{\|\mathbf{s}_p\|^2}{2\,N_0}\,, \quad (22b)$$

respectively.

The probability of error when symbol S_ℓ is transmitted, which we denote as P_{e_ℓ}, is given by

$$\begin{aligned}P_{e_\ell}=\Pr\Bigg[&\frac{2\,\pi\,(\ell-1)}{M}+\frac{\pi}{M}<\text{angle}\left(\hat{\mathbf{h}}^H\mathbf{r}\Big|_{s=S_\ell}\right)\\&<\frac{2\,\pi\,(\ell-1)}{M}+2\,\pi-\frac{\pi}{M}\Bigg]\,.\end{aligned} \quad (23)$$

It is clear from (20) that P_{e_ℓ} is the same for all $\ell=1,2,\ldots,M$. Therefore the symbol error probability P_e is equal to P_{e_ℓ} and can be expressed using (23) and (20) as

$$P_e=\Pr\left(\frac{\pi}{M}<\text{angle}\left((\mathbf{h}+\mathbf{v})^H(\mathbf{h}+\mathbf{u})\right)<2\,\pi-\frac{\pi}{M}\right), \quad (24)$$

with

$$\mathbf{u} \sim \mathcal{CN}\left(\mathbf{0}_L, \frac{1}{\Gamma}\mathbf{I}_L\right), \qquad \mathbf{v} \sim \mathcal{CN}\left(\mathbf{0}_L, \frac{1}{\Gamma_p}\mathbf{I}_L\right). \quad (25)$$

Note that **u**, **v**, and **h** are independent.

Let

$$D = (\mathbf{h}+\mathbf{v})^H(\mathbf{h}+\mathbf{u}) \quad (26a)$$

denote the scaled combiner output and

$$D_1 = \Re(D), \quad D_2 = \Im(D). \quad (26b)$$

Using (2) of Theorem 1, the conditional joint c.f. of D_1 and D_2, conditioned on **h**, is given by

$$\begin{aligned}\Psi_{D_1,D_2|\mathbf{h}}(\jmath\omega_1,\jmath\omega_2|\mathbf{h}) &= \mathbf{E}\left[\exp\left\{\jmath\left(\omega_1 D_1+\omega_2 D_2\right)\right\}|\,\mathbf{h}\right]\\ &= \left(1+\frac{\left(\omega_1^2+\omega_2^2\right)}{4\,\Gamma\,\Gamma_p}\right)^{-L}\\ &\quad\times\exp\left\{-\frac{\left(\omega_1^2+\omega_2^2\right)\,\frac{(\Gamma+\Gamma_p)}{4\,\Gamma\,\Gamma_p}-\jmath\omega_1}{1+\frac{\left(\omega_1^2+\omega_2^2\right)}{4\,\Gamma\,\Gamma_p}}\|\mathbf{h}\|^2\right\}.\end{aligned} \quad (27)$$

By averaging (27) over the statistics of **h** using the c.f. of $\|\mathbf{h}\|^2$, we get

$$\begin{aligned}\Psi_{D_1,D_2}(\jmath\omega_1,\jmath\omega_2) &= \left(1+\frac{\left(\omega_1^2+\omega_2^2\right)}{4\,\Gamma\,\Gamma_p}\right)^{-L}\\ &\quad\times\Psi_{\|\mathbf{h}\|^2}\left(-\frac{\left(\omega_1^2+\omega_2^2\right)\,\frac{(\Gamma+\Gamma_p)}{4\,\Gamma\,\Gamma_p}-\jmath\omega_1}{1+\frac{\left(\omega_1^2+\omega_2^2\right)}{4\,\Gamma\,\Gamma_p}}\right).\end{aligned} \quad (28)$$

A. BPSK

Based on (24) the ABEP of pilot-assisted BPSK can be obtained as $P_e = \Pr\{D_1 < 0\}$ and can be directly evaluated using the Gil-Pelaez inversion theorem [9] as

$$P_e = \frac{1}{2} - \frac{1}{2\,\pi}\int_{-\infty}^{\infty}\frac{1}{\omega}\,\Im\left\{\Psi_{D_1}(\jmath\omega)\right\}\mathrm{d}\omega, \quad (29)$$

with $\Psi_{D_1}(\jmath\omega) = \Psi_{D_1,D_2}(\jmath\omega,0)$ being a marginal c.f. of $\Psi_{D_1,D_2}(\jmath\omega_1,\jmath\omega_2)$.

B. QPSK

In order to obtain the ASEP performance of pilot-assisted QPSK, we consider a $\pi/4$-rotated constellation compared to that considered in (12), i.e., $S_\ell = \sqrt{2\,E_s}\,\exp\{\jmath\,\pi\,(2\,\ell-1)/4\}$ ($\ell = 1, 2, 3, 4$), while (20) is modified as

$$\hat{\mathbf{h}}^H\,\mathbf{r}\Big|_{s=S_\ell} = \sqrt{2\,E_s}\,(\mathbf{h}+\mathbf{v})^H\,\left(\mathbf{h}\,\exp\left\{\jmath\,\frac{\pi}{4}\,(2\,\ell-1)\right\}+\mathbf{u}\right), \quad (30)$$

where $\mathbf{u} = \mathbf{n}/\sqrt{2\,E_s}$ and has a $\mathcal{CN}\left(\mathbf{0}_L, (N_0/E_s)\,\mathbf{I}_L\right)$ distribution which is independent of **v**. Now, $B = (\mathbf{h}+\mathbf{v})^H\,(\mathbf{h}\,\exp\{\jmath\,\pi\,(2\,\ell-1)/4\}+\mathbf{u})$, with $B_1 = \Re\{B\}$ and $B_2 = \Im\{B\}$. Following a similar analysis as before, the joint c.f. of B_1 and B_2 can be derived as

$$\begin{aligned}\Phi_{B_1,B_2}(\jmath\omega_1,\jmath\omega_2) &= \left(1+\frac{\left(\omega_1^2+\omega_2^2\right)}{4\,\Gamma\,\Gamma_p}\right)^{-L}\\ &\quad\times\Psi_{\|\mathbf{h}\|^2}\left(-\frac{\left(\omega_1^2+\omega_2^2\right)\,\frac{(\Gamma+\Gamma_p)}{4\,\Gamma\,\Gamma_p}+\frac{\jmath}{\sqrt{2}}\,(\omega_1+\omega_2)}{1+\frac{\left(\omega_1^2+\omega_2^2\right)}{4\,\Gamma\,\Gamma_p}}\right).\end{aligned} \quad (31)$$

We assume that S_3 is transmitted, and since all symbols S_ℓ are equiprobable, the QPSK ASEP can be calculated as

$$P_e = 1 - \Pr\{B_1 \le 0, B_2 \le 0\}. \quad (32)$$

The joint event in the above equation can be analytically evaluated based on the multivariate inversion theorem [8, eq. (11)] according to which (32) yields

$$\begin{aligned}P_e =& \frac{1}{2\,\pi^2}\int_0^\infty\int_0^\infty\frac{1}{\omega_1\,\omega_2}\,\Re\{\Phi_{B_1,B_2}(\jmath\omega_1,\jmath\omega_2)\\ &-\Phi_{B_1,B_2}(\jmath\omega_1,-\jmath\omega_2)\}\mathrm{d}\omega_1\,\mathrm{d}\omega_2+\frac{5}{4}-\frac{1}{2}\,(P_1+P_2),\end{aligned} \quad (33)$$

with $P_i = \Pr\{B_i \le 0\}$ ($i = 1, 2$) and can evaluated using (29) as $P_i = \frac{1}{2} - \frac{1}{2\,\pi}\int_{-\infty}^{\infty}\frac{1}{\omega}\,\Im\left\{\Phi_{B_i}(\jmath\omega)\right\}\mathrm{d}\omega$. Note that corresponding analytical expressions for QPSK in case of correlated Rice fading can be found in [10] and [11]. In [10] the results are in terms of single integrals, while in [11] they are in terms of the Gauss-Chebyshev quadrature formula. Results for independent Nakagami fading are given in [12].

C. MPSK

Let $\Theta = \mathrm{angle}(D)$ denote the phase of D and $f_{D_1,D_2|\mathbf{h}}(\cdot,\cdot|\mathbf{h})$ the conditional joint p.d.f. of D_1 and D_2, conditioned on **h**. The conditional p.d.f. of Θ, conditioned on **h**, is given by

$$\begin{aligned}f_{\Theta|\mathbf{h}}(\theta|\mathbf{h}) &= \int_0^\infty t f_{D_1,D_2|\mathbf{h}}(t\,\cos\theta, t\,\sin\theta|\mathbf{h})\,dt\\ &= \frac{1}{4\pi^2}\int_{\omega_1=-\infty}^{\infty}\int_{\omega_2=-\infty}^{\infty}\Psi_{D_1,D_2|\mathbf{h}}(\jmath\omega_1,\jmath\omega_2|\mathbf{h})\\ &\quad\times\int_{t=0}^{\infty}t\,\exp\left\{-\jmath\,t\,(\omega_1\,\cos\theta+\omega_2\,\sin\theta)\right\}\,dt\,d\omega_2\,d\omega_1.\end{aligned} \quad (34)$$

We find from (24) that the conditional symbol error probability, conditioned on **h**, is given by

$$P_e(\mathbf{h}) = \int_{\frac{\pi}{M}}^{2\pi-\frac{\pi}{M}} f_{\Theta|\mathbf{h}}(\theta|\mathbf{h})\,d\theta. \quad (35)$$

Substituting (34) in (35), we get

$$\begin{aligned}P_e(\mathbf{h}) &= \frac{1}{4\pi^2}\int_{\omega_1=-\infty}^{\infty}\int_{\omega_2=-\infty}^{\infty}\Psi_{D_1,D_2|\mathbf{h}}(\jmath\omega_1,\jmath\omega_2|\mathbf{h})\\ &\quad\times\int_{\theta=\frac{\pi}{M}}^{2\pi-\frac{\pi}{M}}\int_{t=0}^{\infty}t\,\exp\left\{-\jmath\,t\,(\omega_1\,\cos\theta+\omega_2\,\sin\theta)\right\}\\ &\qquad\times\,dt\,d\theta\,d\omega_2\,d\omega_1.\end{aligned} \quad (36)$$

Changing the variables of integration in (36) from ω_1, ω_2, and t to ρ, ϕ, and η, where

$$\omega_1 = \rho\,\cos\phi, \quad \omega_2 = \rho\,\sin\phi, \quad \eta = \rho\,t, \quad (37)$$

and defining the function $G(\phi, M)$ as

$$G(\phi,M) \triangleq \int_{\theta=\frac{\pi}{M}}^{2\,\pi-\frac{\pi}{M}}\int_{\eta=0}^{\infty}\eta\,\exp\left\{-\jmath\,\eta\,\cos(\theta-\phi)\right\}\,d\eta\,d\theta, \quad (38)$$

yields

$$P_e(\mathbf{h}) = \frac{1}{4\pi^2}\int_{\rho=0}^{\infty}\int_{\phi=-\pi}^{\pi} \Psi_{D_1,D_2|\mathbf{h}}(\jmath\,\rho\,\cos\phi, \jmath\,\rho\,\sin\phi|\mathbf{h}) \times \frac{G(\phi,M)}{\rho}\,d\phi\,d\rho\,. \tag{39}$$

Substituting (27) in (39) we get

$$P_e(\mathbf{h}) = \frac{1}{4\pi^2}\int_{\rho=0}^{\infty}\int_{\phi=-\pi}^{\pi} \exp\left\{-\frac{\frac{\rho^2(\Gamma+\Gamma_p)}{4\,\Gamma\,\Gamma_p} - \jmath\,\rho\,\cos\phi}{1+\frac{\rho^2}{4\,\Gamma\,\Gamma_p}}\|\mathbf{h}\|^2\right\} \times \frac{G(\phi,M)}{\rho\left(1+\frac{\rho^2}{4\,\Gamma\,\Gamma_p}\right)^L}\,d\phi\,d\rho\,. \tag{40}$$

Averaging of $P_e(\mathbf{h})$ over the statistics of $\mathbf{h}$ we get the ASEP of MPSK as

$$P_e = \frac{1}{4\,\pi^2}\int_{\rho=0}^{\infty}\int_{\phi=-\pi}^{\pi} \Psi_{\|\mathbf{h}\|^2}\left(-\frac{\frac{\rho^2(\Gamma+\Gamma_p)}{4\,\Gamma\,\Gamma_p} - \jmath\,\rho\,\cos\phi}{1+\frac{\rho^2}{4\,\Gamma\,\Gamma_p}}\right) \times \frac{G(\phi,M)}{\rho\left(1+\frac{\rho^2}{4\,\Gamma\,\Gamma_p}\right)^L}\,d\phi\,d\rho\,. \tag{41}$$

We now consider two special cases.

1) Perfect CSI: Let us first consider the case of perfect CSI, which implies $\hat{\mathbf{h}} = \mathbf{h}$, and therefore $\Gamma_p \to \infty$. It is well-known that the ASEP in this case is given by

$$P_{e,\,\text{perfect CSI}} = \frac{1}{\pi}\int_0^{\frac{\pi(M-1)}{M}} \Psi_{\|\mathbf{h}\|^2}\left(-\Gamma\,\frac{\sin^2(\pi/M)}{\sin^2\alpha}\right)d\alpha\,. \tag{42}$$

Putting $\Gamma_p \to \infty$ in (41) and comparing the result with (42), we get the following useful identity

$$\frac{1}{4\pi^2}\int_{\rho=0}^{\infty}\int_{\phi=-\pi}^{\pi} \Psi_{\|\mathbf{h}\|^2}\left(-\frac{\rho^2}{4\,\Gamma} + \jmath\,\rho\,\cos\phi\right)\frac{G(\phi,M)}{\rho}\,d\phi\,d\rho = \frac{1}{\pi}\int_0^{\frac{\pi(M-1)}{M}} \Psi_{\|\mathbf{h}\|^2}\left(-\frac{\Gamma\,\sin^2(\pi/M)}{\sin^2\alpha}\right)d\alpha\,. \tag{43}$$

2) High SNR Approximation: We now consider that the case of high SNR when $\Gamma \gg 1$ and $\Gamma_p \gg 1$. From (41), we obtain

$$P_{e,\,\text{high SNR}} \approx \frac{1}{4\pi^2}\int_{\rho=0}^{\infty}\int_{\phi=-\pi}^{\pi} \Psi_{\|\mathbf{h}\|^2}\left(-\rho^2\,\frac{\Gamma+\Gamma_p}{4\,\Gamma\,\Gamma_p} + \jmath\,\rho\,\cos\phi\right) \times \frac{G(\phi,M)}{\rho}\,d\phi\,d\rho\,. \tag{44}$$

Replacing Γ with $\Gamma\,\Gamma_p/(\Gamma+\Gamma_p)$ in the identity (43) and applying the result to (44), we obtain a high SNR ASEP approximate expression

$$P_{e,\,\text{high SNR}} \approx \frac{1}{\pi}\int_0^{\frac{\pi(M-1)}{M}} \Psi_{\|\mathbf{h}\|^2}\left(-\frac{\Gamma\,\Gamma_p}{\Gamma+\Gamma_p}\,\frac{\sin^2\left(\frac{\pi}{M}\right)}{\sin^2\alpha}\right)d\alpha\,. \tag{45}$$

Obviously, for $\Gamma_p \to \infty$, the above expression agrees with (42). Furthermore, as $\Gamma \to \infty$, P_e becomes independent of Γ and an error floor is formed.

V. Optimal Pilot Symbol Power Allocation

We now derive the optimal power allocated by the pilot symbols. The L fading channels are considered as block, while in order to satisfy the conditions for the Nyquist sampling theorem, the maximum frame duration, that is the time duration between two successive pilot symbols, must be not higher than $T_f = 1/(2\,f_D)$, with f_D being the maximum Doppler frequency shift. Denoting as T_s the MPSK symbols' duration, the channel block length is $W = \lfloor T_f/T_s \rceil = \lfloor 1/(2\,f_D\,T_s) \rceil$, where $\lfloor\cdot\rceil$ stands for the closest rounded-down positive integer.

Consider the case of high SNR, i.e., when $\Gamma \gg 1$ and $\Gamma_p \gg 1$. We find from Section IV-C2 that the error performance in this case depends explicitly only on the argument $1/\Gamma + 1/\Gamma_p$ in (45). By denoting as γ_p the power of each pilot symbol, i.e., $\gamma_p = \Gamma_p/K$, the pilot-to-data symbol power ratio is defined as $\chi \triangleq \gamma_p/\Gamma$. Moreover, we define the *effective SNR per symbol* as

$$\gamma_{\text{eff}} = \frac{(W-K)\,\Gamma + K\,\gamma_p}{W-K}\,. \tag{46}$$

Using the aforementioned definitions, $1/\Gamma + 1/\Gamma_p$ can be expressed as a function of χ and K as

$$\frac{1}{\Gamma}+\frac{1}{\Gamma_p} = \underbrace{\left(1+\frac{\chi\,K}{W-K}\right)\left(1+\frac{1}{\chi\,K}\right)}_{\Xi(\chi,K)}\frac{1}{\gamma_{\text{eff}}} = \Xi(\chi,K)\,\frac{1}{\gamma_{\text{eff}}}\,. \tag{47}$$

In order to minimize P_e in (45), the above equation should be minimized. This can be succeeded by minimizing $\Xi(\chi,K)$ with respect to χ or K. For fixed χ, the optimum K can be obtained finding the root of $\partial\Xi/\partial K = 0$ with respect to K as

$$K_{\text{opt}} = \left\lfloor \frac{W}{\sqrt{W\,\chi^2+\chi}+1} \right\rceil\,. \tag{48a}$$

When $\chi = 1$, (48a) simplifies as $K_{\text{opt}} = \left\lfloor\sqrt{1+W}\right\rceil - 1$. Moreover, for fixed K, the optimum χ can be obtained finding the root of $\partial\Xi/\partial\chi = 0$ with respect to χ as

$$\chi_{\text{opt}} = \frac{\sqrt{W-K}}{K}\,. \tag{48b}$$

When $K = 1$, (48b) simplifies as $\chi_{\text{opt}} = \sqrt{W-1}$. Clearly, the optimal values are independent of the correlation model and the number of diversity branches.

VI. MPSK ASEP Performance over Nakagami and Rice Fading

Let $\mathbf{h}$ be the channel gain vector normalized so that

$$\frac{1}{L}\,\text{tr}\left(\mathbf{E}\left[\mathbf{h}\,\mathbf{h}^H\right]\right) = \frac{1}{L}\,\mathbf{E}\left[\|\mathbf{h}\|^2\right] = 1 \tag{49}$$

and $\mathbf{K}_h = \mathbf{E}[(\mathbf{h}-\mathbf{m}_h)(\mathbf{h}-\mathbf{m}_h)^H]$ be its *normalized channel covariance matrix*, with $\mathbf{m}_h = \mathbf{E}[\mathbf{h}]$. Let $\epsilon_1, \epsilon_2, \ldots, \epsilon_N$ denote the N distinct eigenvalues of $\mathbf{K}_h$, having multiplicity q_i for $i = 1, 2, \ldots, N$, with $\sum_{i=1}^N q_i = L$, while owing to the positive definiteness of $\mathbf{K}_h$, $\epsilon_1, \epsilon_2, \ldots, \epsilon_N$ are real and positive.

A. Nakagami Fading

When $\mathbf{h}$ is subject to Nakagami fading, $\mathbf{K}_h$ has the form

$$\mathbf{K}_h = \frac{1}{m}\begin{pmatrix} 1 & \rho_{12} & \cdots & \rho_{1L} \\ \rho_{21} & 1 & \cdots & \rho_{2L} \\ \vdots & \vdots & \ddots & \vdots \\ \rho_{L1} & \rho_{L2} & \cdots & 1 \end{pmatrix}, \tag{50}$$

with m being the Nakagami fading parameter and ρ_{ij} being the correlation coefficient between ith and jth channels of the underlying Gaussian processes ($i, j = 1, 2, \ldots, L$). Owing to (49), $\mathbf{K}_h$ satisfies the condition $\mathrm{tr}\,(\mathbf{K}_h) = L/m$, while $\sum_{i=1}^{N} q_i\,\epsilon_i = L/m$. The c.f. of $\|\mathbf{h}\|^2$ is

$$\Psi_{\|\mathbf{h}\|^2}(\jmath\,\omega) = \frac{1}{\det\left(\mathbf{I}_L - \jmath\,\omega\,\mathbf{K}_h\right)^m} = \frac{1}{\prod_{i=1}^{N}\left(1-\jmath\,\omega\,\epsilon_i\right)^{m\,q_i}}. \tag{51}$$

1) ASEP for MPSK with $M \geq 2$: For $M \geq 2$, substituting (51) in (41), we get

$$P_e = \frac{1}{4\pi^2}\int_{\rho=0}^{\infty}\int_{\phi=-\pi}^{\pi}\left(1+\frac{\rho^2}{4\,\Gamma\,\Gamma_p}\right)^{(m-1)\,L} \times \frac{1}{\rho\prod_{i=1}^{N}\left(1-\jmath\,\rho\,\epsilon_i\,\cos\phi+\frac{\rho^2\left(\left(\Gamma+\Gamma_p\right)\,\epsilon_i+1\right)}{4\,\Gamma\,\Gamma_p}\right)^{m\,q_i}} \times G(\phi, M)\,d\phi\,d\rho\,. \tag{52}$$

When $M > 2$, further simplification of the above expression is extremely difficult even for Rayleigh fading.

For integer m and using (45), (51), [14, Appendix C, eq. (5A.70)], and the Appendix, a high-SNR approximate expression yields as

$$P_{e,\,\text{high SNR}} = \sum_{i=1}^{N}\sum_{k=1}^{m\,q_i} A_{ik}\,\mathcal{S}_k\left(\epsilon_i\,\frac{\Gamma\,\Gamma_p}{\left(\Gamma+\Gamma_p\right)}\,\sin^2\left(\frac{\pi}{M}\right)\right), \tag{53}$$

where

$$A_{i,k} = \frac{c_i^{-m\,q_i+k}}{(m\,q_i-k)!}\,\frac{\partial^{m\,q_i-k}}{\partial x^{m\,q_i-k}}\,\prod_{\substack{t=1\\ t\neq i}}^{N}\left(1+c_t\,x\right)^{-m\,q_t}\Bigg|_{x=-1/c_i}, \tag{54}$$

with $c_i = \epsilon_i\,\frac{\Gamma\,\Gamma_p}{\Gamma+\Gamma_p}\,\sin^2\left(\frac{\pi}{M}\right)$. Note that the multiple derivatives in (54) can be computed using the Faa di Bruno's formula [15], while also note that (53) consists only of elementary functions.

2) ASEP for QPSK: For $M = 4$ substituting (51) in (33), the ASEP of QPSK can be extracted in terms of a two-fold integral.

3) ABEP for BPSK: Using (28) and (51), the joint c.f. of D_1 and D_2 yields

$$\Psi_{D_1,D_2}\left(\jmath\,\omega_1,\jmath\,\omega_2\right) = \left(1+\frac{\omega_1^2+\omega_2^2}{4\,\Gamma\,\Gamma_p}\right)^{(m-1)\,L} \times\prod_{i=1}^{N}\left(1-\jmath\,\omega_1\,\epsilon_i+\left(\omega_1^2+\omega_2^2\right)\,\frac{\left(\Gamma+\Gamma_p\right)\,\epsilon_i+1}{4\,\Gamma\,\Gamma_p}\right)^{-m\,q_i}. \tag{55}$$

For $M = 2$ (case of BPSK) and based on Section IV-A, the ABEP can be obtained directly from the c.f. of D_1, which is

$$\Psi_{D_1}(\jmath\,\omega_1) = \left(1+\frac{\omega_1^2}{4\,\Gamma\,\Gamma_p}\right)^{(m-1)\,L} \times\prod_{i=1}^{N}\left(1-\jmath\,\omega_1\,\epsilon_i+\frac{\omega_1^2\left(\left(\Gamma+\Gamma_p\right)\,\epsilon_i+1\right)}{4\,\Gamma\,\Gamma_p}\right)^{-m\,q_i}. \tag{56}$$

This can be expressed as

$$\Psi_{D_1}(z) = \frac{\left(1-\frac{z^2}{4\,\Gamma\,\Gamma_p}\right)^{(m-1)\,L}}{\prod_{i=1}^{N}\left(1-z\,\lambda_{i1}\right)^{m\,q_i}\left(1-z\,\lambda_{i2}\right)^{m\,q_i}}, \tag{57}$$

where

$$\lambda_{i1} = \frac{\epsilon_i}{2}\left(1+\sqrt{1+\frac{\left(\Gamma+\Gamma_p\right)\,\epsilon_i+1}{\Gamma\,\Gamma_p\,\epsilon_i^2}}\right) \tag{58a}$$

and

$$\lambda_{i2} = \frac{\epsilon_i}{2}\left(1-\sqrt{1+\frac{\left(\Gamma+\Gamma_p\right)\,\epsilon_i+1}{\Gamma\,\Gamma_p\,\epsilon_i^2}}\right). \tag{58b}$$

Here $\lambda_{i1} > 0$ and $\lambda_{i2} < 0$. For integer values of m, $\Gamma \neq \Gamma_p$, and from the inversion theorem [9], the ABEP is the negative of the sum of residues of $\Psi_{D_1}(z)/z$ at poles on the left-half z-plane [13], that is, at $z = 1/\lambda_{i2}$, $i = 1, 2, \ldots, N$, and can be expressed in closed form as given by (59a) and shown on the top of the next page, where the composite summation is performed over all possible $(m\,q_j - 1)$-tuples $(l_1, l_2, \ldots, l_{m\,q_j-1})$ of integers in $[0, m\,q_j - 1]$ satisfying $\sum_{n=1}^{m\,q_j-1} n\,l_n = m\,q_j - 1$. Also, using (57) with $\Gamma = \Gamma_p$, and following a similar procedure as that for (59a), a corresponding ABEP expression is obtained given by (59b) as shown on the top of the next page. For $m = 1$ (59a) simplifies to the ABEP expression for Rayleigh fading, that is also valid for $\Gamma = \Gamma_p$.

B. Rice Fading

Let the channel be subject to Rice fading with the channel gain vector $\mathbf{h}$ having a $\mathcal{CN}(\mathbf{m}_h, \mathbf{K}_h)$ distribution. Owing to (49), the average channel gain vector is $\mathbf{m}_h = \left[\sqrt{\frac{\mathcal{K}_1}{1+\mathcal{K}_1}}\,\sqrt{\frac{\mathcal{K}_2}{1+\mathcal{K}_2}}\cdots\sqrt{\frac{\mathcal{K}_L}{1+\mathcal{K}_L}}\right] \times\exp\{\jmath\,\mathbf{Q}\}$, with $\mathcal{K}_i \geq 0$ being the Rice K-factor of the ith channel and $\mathbf{Q}$ being the phase of $\mathbf{m}_h$. Also, $\mathbf{K}_h$ has the form

$$\mathbf{K}_h = \begin{pmatrix} \frac{1}{1+\mathcal{K}_1} & \frac{\rho_{12}}{\sqrt{1+\mathcal{K}_1}\sqrt{1+\mathcal{K}_2}} & \cdots & \frac{\rho_{1L}}{\sqrt{1+\mathcal{K}_1}\sqrt{1+\mathcal{K}_L}} \\ \frac{\rho_{21}}{\sqrt{1+\mathcal{K}_2}\sqrt{1+\mathcal{K}_1}} & \frac{1}{1+\mathcal{K}_2} & \cdots & \frac{\rho_{2L}}{\sqrt{1+\mathcal{K}_2}\sqrt{1+\mathcal{K}_L}} \\ \vdots & \vdots & \ddots & \vdots \\ \frac{\rho_{L1}}{\sqrt{1+\mathcal{K}_L}\sqrt{1+\mathcal{K}_1}} & \frac{\rho_{L2}}{\sqrt{1+\mathcal{K}_L}\sqrt{1+\mathcal{K}_2}} & \cdots & \frac{1}{1+\mathcal{K}_L} \end{pmatrix}, \tag{61}$$

satisfying the condition

$$\mathrm{tr}\,(\mathbf{K}_h) = \sum_{i=1}^{L}\frac{1}{1+\mathcal{K}_i}, \tag{62}$$

while from (62), we have $\sum_{i=1}^{N} q_i\,\epsilon_i = \sum_{i=1}^{L}(1+\mathcal{K}_i)^{-1}$. Moreover, $\mathbf{K}_h$ can be decomposed as $\mathbf{K}_h = \mathbf{B}_h\,\mathbf{Q}_h\,\mathbf{B}_h^H$, with

$$P_{e,\Gamma\neq\Gamma_p}=\sum_{j=1}^{N}\frac{(-\lambda_{j2})^{2\,m\,L-m\,q_j}}{\left[\prod_{i=1}^{N}(\lambda_{i1}-\lambda_{j2})^{m\,q_i}\right]\prod_{\substack{i=1\\ i\neq j}}^{N}(\lambda_{i2}-\lambda_{j2})^{m\,q_i}}\left(1-\frac{1}{4\,\Gamma\,\Gamma_p\,\lambda_{j2}^2}\right)^{(m-1)\,L}$$
$$\times\sum_{\substack{l_1,l_2,\ldots,l_{m\,q_j-1}=0\\ 0\le l_1,\ldots,l_{m\,q_j-1}\le m\,q_j-1\\ l_1+2l_2+\cdots+(m\,q_j-1)l_{m\,q_j-1}=m\,q_j-1}}\prod_{n=1}^{m\,q_j-1}\frac{n^{-l_n}}{l_n!}\left[1-(m-1)\,L\left(\frac{1}{\left(1-\sqrt{4\,\Gamma\,\Gamma_p}\,\lambda_{j2}\right)^n}+\frac{1}{\left(1+\sqrt{4\,\Gamma\,\Gamma_p}\,\lambda_{j2}\right)^n}\right)\right.$$
$$\left.+m\sum_{i=1}^{N}\frac{q_i\lambda_{i1}^n}{(\lambda_{i1}-\lambda_{j2})^n}+m\sum_{\substack{i=1\\ i\neq j}}^{N}\frac{q_i\lambda_{i2}^n}{(\lambda_{i2}-\lambda_{j2})^n}\right]^{l_n} \tag{59a}$$

$$P_{e,\Gamma=\Gamma_p}=\frac{2^{-L}}{\prod_{i=1}^{N}(1+\epsilon_i\,\Gamma)^{m\,q_i}}\sum_{\substack{l_1,l_2,\ldots,l_{L-1}=0\\ 0\le l_1,\ldots,l_{L-1}\le L-1\\ l_1+2l_2+\cdots+(L-1)l_{L-1}=L-1}}\prod_{n=1}^{L-1}\frac{n^{-l_n}}{l_n!}\left[1-\frac{(m-1)\,L}{2^n}+m\sum_{i=1}^{N}q_i\left(\frac{\epsilon_i\,\Gamma+0.5}{\epsilon_i\,\Gamma+1}\right)^n\right]^{l_n} \tag{59b}$$

$\mathbf{B}_h$ being the orthonormal eigenvectors matrix of $\mathbf{K}_h$ and $\mathbf{Q}_h$ the corresponding diagonal matrix of eigenvalues of $\mathbf{K}_h$. The c.f. of $\|\mathbf{h}\|^2$ is given by

$$\Psi_{\|\mathbf{h}\|^2}(\jmath\,\omega)=\frac{\exp\left\{-\mathbf{m}_h^H\left[\mathbf{K}_h-\frac{1}{\jmath\,\omega}\,\mathbf{I}_L\right]^{-1}\mathbf{m}_h\right\}}{\det\left(\mathbf{I}_L-\jmath\,\omega\,\mathbf{K}_h\right)}$$
$$=\frac{1}{\prod_{i=1}^{N}(1-\jmath\,\omega\,\epsilon_i)^{q_i}}\,\exp\left\{\sum_{k=1}^{L}\frac{|b_k|^2}{(\jmath\,\omega)^{-1}-\epsilon_k}\right\}, \tag{63}$$

with vector $\mathbf{b}=[b_1\,b_2\cdots b_L]^T$ given by $\mathbf{b}=\mathbf{B}_h^H\,\mathbf{m}_h$ and $\epsilon_{N+1},\epsilon_{N+2},\ldots,\epsilon_L$ being repeats of the $\epsilon_1,\epsilon_2,...,\epsilon_N$ with appropriate multiplicities.

Using (45) and (63) a high SNR approximate ASEP expression for MPSK can be easily extracted for any correlation matrix. Below we specifically provide high-SNR approximate expressions for two important special cases.

1) Constant Correlation: Assuming constant correlation among all channels, i.e., for $i=j$, $[\mathbf{K}_h]_{ij}=1/(1+\mathcal{K})$, while for $i\neq j$, $[\mathbf{K}_h]_{ij}=\rho/(1+\mathcal{K})$ $\forall i,j=1,2,\ldots,L$, with $\mathcal{K}_i=\mathcal{K}$ $\forall i=1,2,\ldots,L$, a simplified expression can be obtained, setting $N=2$, $\epsilon_1=(1-\rho)/(1+\mathcal{K})$, $\epsilon_2=(1+\rho\,(L-1))/(1+\mathcal{K})$, and $q_1=L-1$, $q_2=1$, as

$$P_{e,\text{ high SNR}}=\frac{1}{\pi}\sum_{i=1}^{2}\sum_{k=1}^{q_i}A_{ik}$$
$$\times\int_0^{\frac{\pi(M-1)}{M}}\left(1+\frac{\Gamma\,\Gamma_p}{\Gamma+\Gamma_p}\,\epsilon_i\,\frac{\sin^2(\pi/M)}{\sin^2(\alpha)}\right)^{-k}$$
$$\times\exp\left\{-\frac{L\,\mathcal{K}}{1+(L-1)\,\rho+(1+\mathcal{K})\,\frac{\Gamma+\Gamma_p}{\Gamma\,\Gamma_p}\,\frac{\sin^2(a)}{\sin^2(\pi/M)}}\right\}d\alpha\,. \tag{64}$$

For Rayleigh fading ($\mathcal{K}=0$) and using the Appendix, the above expression is in agreement with (53) when $m=1$.

2) I.I.D. Fading: In the special case of i.i.d. fading with $\mathbf{K}_h=\text{diag}((1+\mathcal{K}_1)^{-1},(1+\mathcal{K}_2)^{-1},\ldots,(1+\mathcal{K}_L)^{-1})$, we have $\epsilon_i=(1+\mathcal{K}_i)^{-1}$, $\forall i=1,2,\ldots,L$. From (63), the ASEP can be expressed by (65), as shown on the top of the next page. Assuming that Γ, $\Gamma_p\gg 1$, replacing Γ with $\Gamma\,\Gamma_p/(\Gamma+\Gamma_p+1)$ in the identity (43), and applying the result to (65), yields (66), as shown on the top of the next page. Although (66) is a high-SNR approximate ASEP formula for Rice fading, for the special case of Rayleigh fading, i.e., setting $\mathcal{K}_i=0$, the resulting formula is exact under the reasonable assumption $\Gamma+\Gamma_p\gg 1$, while using the Appendix can be further expressed in closed form as

$$P_{e,\text{ i.i.d.}}=\mathcal{S}_L\left(\frac{\Gamma\,\Gamma_p}{(\Gamma+\Gamma_p+1)}\,\sin^2\left(\frac{\pi}{M}\right)\right). \tag{67}$$

VII. Numerical and Computer Simulation Results

Fig. 1 shows plots of the ASEP of QPSK for Rayleigh fading versus the average SNR per branch and per symbol, Γ, with different values of the average PNR per symbol, $\Gamma_p=5$, 10, 15, 20 dB, and the number of branches $L=2$, 4. Exponentially correlated fading is considered according to which $\rho_{i,j}=\rho^{|i-j|}$ with $\rho=0.5$, where ρ is the *exponential fading power correlation coefficient* and satisfies $-1\le\rho<1$. We find that the exact ASEPs (obtained from (33)) approach the approximate high SNR ASEPs (obtained from (45)) as Γ or Γ_p becomes large. A comparison of the ASEP curves for $L=2$ with those for $L=4$ reveals how the degradation in performance due to imperfect channel estimation can be compensated by increasing the number of receive diversity branches.

In Fig. 2 using (59) or (29) and (45) we plot, respectively, the exact and high SNR approximate ABEPs of BPSK for triple-branch ($L=3$) Nakagami fading with $m=2$, $\rho=0$, 0.5, 0.9, and $\Gamma_p=10$, 20 dB. It is clearly shown that as Γ_p increases the performance improves, while when $\Gamma_p\to\infty$ and/or $\Gamma\to\infty$, the exact and high SNR approximate curves

$$P_e = \frac{1}{4\,\pi^2}\int_{\rho=0}^{\infty}\int_{\phi=-\pi}^{\pi} \frac{\exp\left\{-\sum_{l=1}^{L}\frac{\mathcal{K}_l}{1+\mathcal{K}_l}\left(\frac{1}{1+\mathcal{K}_l}+\frac{1}{-\rho^2\,\frac{\Gamma+\Gamma_p}{4\,\Gamma\,\Gamma_p}+\jmath\,\rho\,\cos\phi}\right)^{-1}\right\}}{\rho\left(1-\jmath\,\rho\,\cos\phi+\frac{\rho^2(\Gamma+\Gamma_p+1)}{4\,\Gamma\,\Gamma_p}\right)^{L}} G(\phi,M)\,d\phi\,d\rho \tag{65}$$

$$P_{e,\,\text{i.i.d.}} \approx \frac{1}{\pi}\int_{0}^{\frac{\pi(M-1)}{M}} \frac{\exp\left\{-\sum_{i=1}^{L}\frac{\mathcal{K}_i}{1+\mathcal{K}_i}\left(\frac{1}{1+\mathcal{K}_i}+\frac{\Gamma+\Gamma_p+1}{\Gamma\,\Gamma_p}\,\frac{\sin^2(\alpha)}{\sin^2(\pi/M)}\right)^{-1}\right\}}{\prod_{i=1}^{N}\left(1+\epsilon_i\,\frac{\Gamma\,\Gamma_p}{\Gamma+\Gamma_p+1}\,\frac{\sin^2(\pi/M)}{\sin^2(\alpha)}\right)^{q_i}}\,d\alpha \tag{66}$$

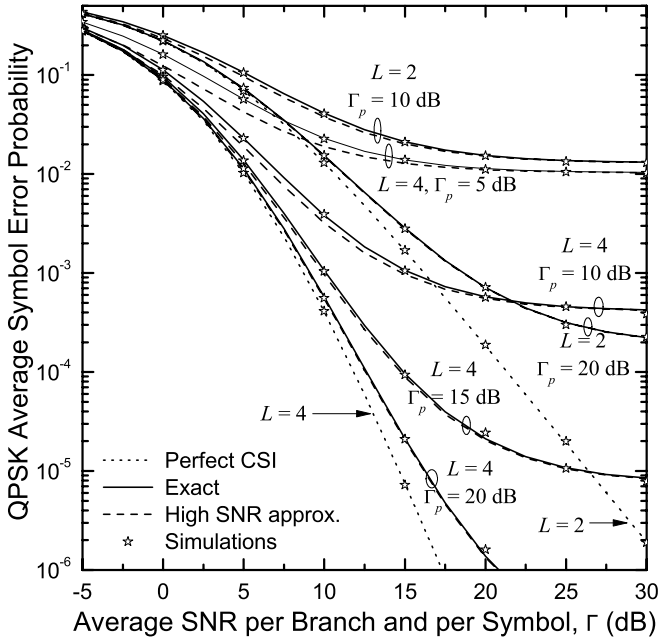

Fig. 1. ASEP of QPSK versus average SNR per branch and per symbol, Γ, for Rayleigh fading and different values of average PNR, Γ_p, and number of branches L.

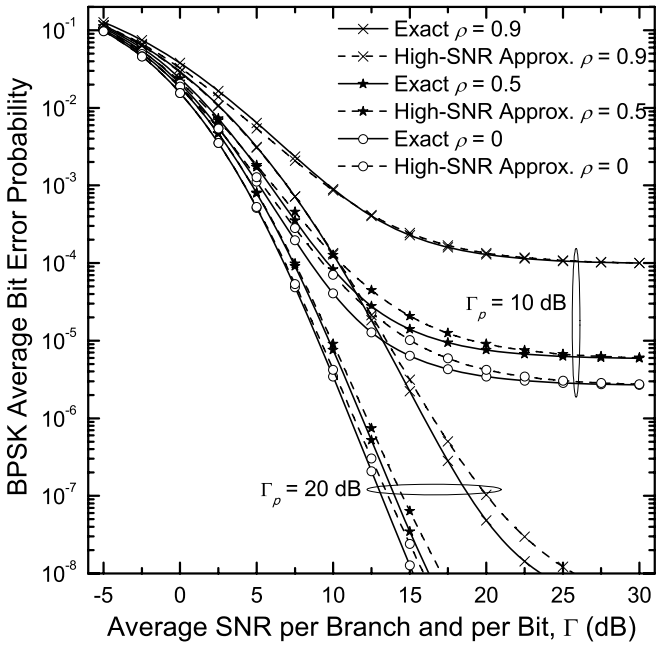

Fig. 2. ABEP of BPSK versus average SNR per branch and per bit, Γ, for triple-branch Nakagami fading with $m = 2$ and exponential correlation with various values of ρ, and for two different values of the average PNR, Γ_p.

coincide. Moreover, the higher the correlation coefficient is, the worse performance is observed. It is also shown that an increased Γ_p can serve as countermeasure on the effect of high correlation channel scenario. In Fig. 3 both exact and high SNR approximate ABEP curves for BPSK are plotted for the same set of values of L, correlation model, and ρ as that in Fig. 2 and also for $\Gamma_p = 10$ dB, and $m = 1, 4$. For fixed Γ, the higher m and/or the lower ρ, the better performance is obtained.

In Fig. 4 we plot ASEP curves (using (64)) for QPSK signaling, $f_D\,T_s = 0.02$, Jakes power spectrum, Rice fading with $L = 3$ and $\mathcal{K} = 1$, 10, and assuming *constant fading power correlation coefficient* according to which $\rho_{i,j} = \rho = 0.5$, $\forall i \neq j = 1, 2, 3$. In this figure we compare curves corresponding to optimal pilot power allocation ($K = 1$ and $\chi_{\text{opt}} = 5$) with the ones for perfect CSI. As shown for fixed $\mathcal{K}$ there is a constant SNR difference between the curves of the two cases that is $\Xi(5, 1) = 1.75$ dB. It can be also verified that for a lower $f_D\,T_s$ product (slower fading channel), the SNR difference between optimal pilot power allocation and perfect CSI becomes lower. In the same figure curves for the ASEP of differentially coherent QPSK (DQPSK) are presented for comparison with corresponding curves for pilot assisted QPSK with optimal power allocation. For $P_{se} = 10^{-4}$, we observe SNR differences about 5 and 3 dB for Rice factor $\mathcal{K} = 1$ and 10, respectively. These differences further increase as the SNR increases showing that pilot assisted coherent systems, assuming an ideal CSI method[1] (see the next paragraph), are more performance beneficial compared to differentially coherent ones.

In order to verify the correctness of the proposed analysis, in Figs. 1, 3, and 4, Monte Carlo computer simulation results, denoted with star signs, are included for Rayleigh/Rice[2] fading and perfect match is observed between them and the analytical results. The method we have used to estimate the channel samples is a fast Fourier transform (FFT)-based one, that is an ideal channel estimation method. Specifically, a low pass interpolator of sinc type impulse response and infinite-length

[1]Note that for a practical channel estimation method with small buffer size interpolator, a further performance degradation has to be taken into consideration [16].

[2]Note that for Nakagami fading we do not have have simulation results since we are not aware of any method that generates multivariate Nakagami envelopes having a specific Doppler power spectrum, e.g., the Jakes one.

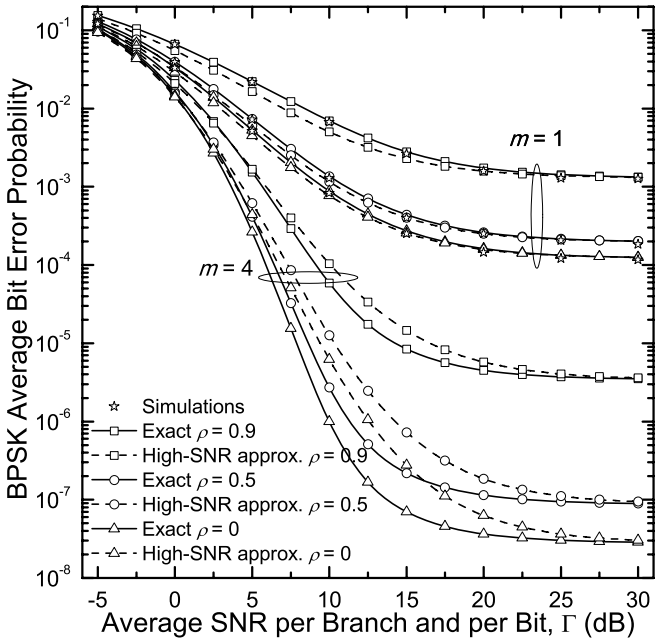

Fig. 3. ABEP of BPSK versus average SNR per branch and per bit, Γ, for triple-branch Nakagami fading, two different values of m, exponential correlation with different values of ρ and $\Gamma_p = 10$ dB.

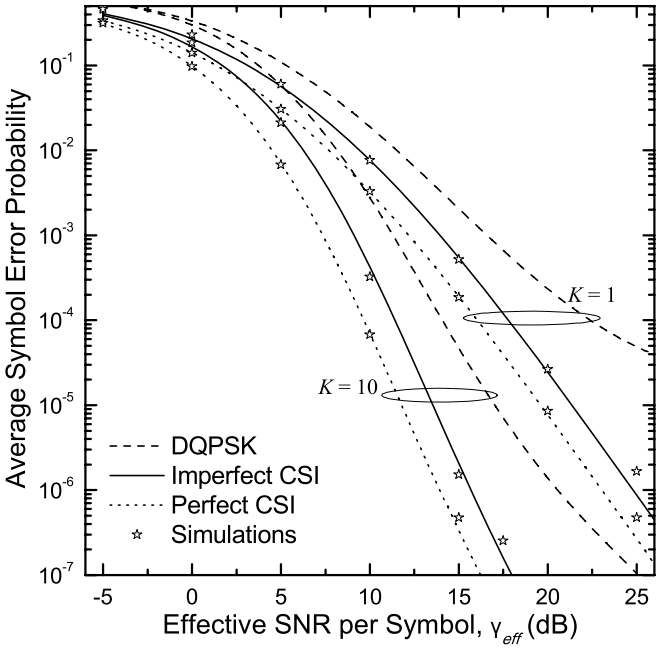

Fig. 4. ASEP of QPSK and DQPSK versus effective SNR per branch, γ_{eff}, for triple-branch Rice fading with different values of $\mathcal{K}$, constant correlation with $\rho = 0.5$, and $f_D\, T_s = 0.02$.

buffer size was implemented. In time domain, this method interpolates the samples between successive pilot symbols with frame duration $T_f = 1/(2f_D)$. More specifically, after extracting from the pilot symbols a vector with channel estimates, we pad $W-1$ zeros between successive estimates. Then, we perform FFT and zeroing all spectrum values for frequencies higher than f_D. Finally, we perform inverse FFT (IFFT) and we get the interpolated channel estimates.

VIII. Conclusions

The error performance of MPSK with MRC using imperfect channel estimates can be conveniently analyzed from the distribution of the inner product of two complex Gaussian vectors having equal means. Therefore, we have first proved a useful theorem concerning the joint c.f. of the real and imaginary parts of the inner product of two complex Gaussian vectors and have then developed a unified analytical framework for the derivation of the ASEP performance of such systems. The receiver is assumed to perform least squares channel estimation by transmitting pilot symbols. For Nakagami fading, closed form ASEP expressions have been obtained for the cases of high SNR and BPSK signaling, while approximate expressions in terms of a single integral have been obtained for Rice fading under the constant correlation model and for i.i.d. channels. In addition, the optimal average pilot-to-noise power ratio has been obtained in closed form. Our findings show that the actual ASEP values approach the approximate high SNR ones as Γ and/or Γ_p becomes large. Comparisons among the ASEP curves reveal how the degradation in performance due to imperfect CSI can be compensated by increasing the number of receive diversity branches. Finally, it has been demonstrated that pilot assisted coherent MPSK systems are more performance beneficial compared to corresponding differentially coherent ones.

Appendix

The closed form solution of

$$\mathcal{S}_k(c) = \frac{1}{\pi}\int_0^{\pi\frac{M-1}{M}} \left(\frac{\sin^2(\alpha)}{\sin^2(\alpha)+c}\right)^k d\alpha \tag{68}$$

is given by [14, Appendix C, eq. (5A.16)]

$$\begin{aligned}\mathcal{S}_k(c) =& \frac{M-1}{M} - \frac{1}{\pi}\sqrt{\frac{c}{c+1}} \\ &\times \left\{ \left(\frac{\pi}{2} + \tan^{-1}(a)\right) \sum_{n=0}^{k-1} \binom{2n}{n} (4(1+c))^{-n} \right. \\ &+ \sin\left(\tan^{-1}(a)\right) \sum_{n=1}^{k-1}\sum_{i=1}^{n} \frac{T_{i,n}}{(1+c)^n} \\ &\left. \times \left[\cos\left(\tan^{-1}(a)\right)\right]^{2(n-1)+1} \right\}\end{aligned} \tag{69}$$

with $a = \cot(\pi/M)\sqrt{c/(1+c)}$ and

$$T_{i,n} = \frac{\binom{2n}{n}}{\binom{2(n-1)}{n-i} 4^i [2(n-i)+1]}.$$

References

[1] J. G. Proakis, "Probabilities of error for adaptive reception of M-phase signals," *IEEE Trans. Commun.*, vol. COM-16, no. 1, pp. 71–81, Feb. 1968.

[2] R. F. Pawula, S. O. Rice, and J. H. Roberts, "Distribution of the phase angle between two vectors perturbed by Gaussian noise," *IEEE Trans. Commun.*, vol. COM-30, no. 8, pp. 1828–1841, Aug. 1982.

[3] R. F. Pawula, "Distribution of the phase angle between two vectors perturbed by Gaussian noise II," *IEEE Trans. Veh. Technol.*, vol. 50, no. 2, pp. 576–583, Mar. 2001.

[4] W. M. Gifford, M. Z. Win, and M. Chiani, "Diversity with practical channel estimation," *IEEE Trans. Wireless Commun.*, vol. 4, no. 4, pp. 1935–1947, July 2005.
[5] Y. Ma, R. Schober, and S. Pasupathy, "Effect of channel estimation errors on MRC diversity in Rician fading channels," *IEEE Trans. Veh. Technol.*, vol. 54, no. 6, pp. 2137–2142, Nov. 2005.
[6] R. You, H. Li, and Y. Bar-Ness, "Diversity combining with imperfect channel estimation," *IEEE Trans. Commun.*, vol. 53, no. 10, pp. 1655–1662, Oct. 2005.
[7] Y. Peng, S. Cui, and R. You, "Optimal pilot-to-data power ratio for diversity combining with imperfect channel estimation," *IEEE Commun. Lett.*, vol. 10, no. 2, pp. 97–99, Feb. 2006.
[8] N. Shephard, "From characteristic function to distribution function: a simple framework for the theory," *Econometric Theory*, vol. 7, pp. 519–529, 1991.
[9] J. Gil-Pelaez, "Note on the inversion theorem," *Biometrika*, vol. 38, pp. 481–482, 1951.
[10] L. Najafizadeh and C. Tellambura, "BER analysis of arbitrary QAM for MRC diversity with imperfect channel estimation in generalized Ricean fading channels," *IEEE Trans. Veh. Technol.*, vol. 55, no. 4, pp. 1239–1248, July 2006.
[11] Y. Ma, R. Schober, and D. Zhang, "Exact BER for M-QAM with MRC and imperfect channel estimation in Rician fading channels," *IEEE Trans. Wireless Commun.*, vol. 6, no. 3, pp. 926–936, Mar. 2007.
[12] Y. Ma and J. Jin, "Effect of channel estimation errors on M-QAM with MRC and EGC in Nakagami fading channels," *IEEE Trans. Veh. Technol.*, vol. 56, no. 3, pp. 1239–1250, May 2007.
[13] P. Garg, R. K. Mallik, and H. M. Gupta, "Performance analysis of space-time coding with imperfect channel estimation," *IEEE Trans. Wireless Commun.*, vol. 4, no. 1, pp. 257–265, Jan. 2005.
[14] M. K. Simon and M.-S. Alouini, *Digital Communication over Fading Channels*, 2nd edition. Wiley, 2005.
[15] C.-J. de la Vallee Poussin, *Cours D'Analyse Infinitesimale*, 12th edition. Gauthier-Villars, Libraire Universitaire Louvain, vol. 1, 1959.
[16] J. M. Torrance and L. Hanzo, "Comparative study of pilot symbol assisted modem schemes," in *Proc. IEE Radio Receivers Associated Syst. Conf.*, Sept. 1995.

Ranjan K. Mallik (S'88–M'93–SM'02) received the B.Tech. degree from the Indian Institute of Technology, Kanpur, in 1987 and the M.S. and Ph.D. degrees from the University of Southern California, Los Angeles, in 1988 and 1992, respectively, all in Electrical Engineering. From August 1992 to November 1994, he was a scientist at the Defence Electronics Research Laboratory, Hyderabad, India, working on missile and EW projects. From November 1994 to January 1996, he was a faculty member of the Department of Electronics and Electrical Communication Engineering, Indian Institute of Technology, Kharagpur. From January 1996 to December 1998, he was with the faculty of the Department of Electronics and Communication Engineering, Indian Institute of Technology, Guwahati. Since December 1998, he has been with the faculty of the Department of Electrical Engineering, Indian Institute of Technology, Delhi, where he is currently a Professor. His research interests are in diversity combining and channel modeling for wireless communications, space-time systems, cooperative communications, multiple-access systems, difference equations, and linear algebra.

Dr. Mallik is a member of Eta Kappa Nu. He is also a member of the IEEE Communications, Information Theory, and Vehicular Technology Societies, the American Mathematical Society, and the International Linear Algebra Society, a fellow of the Indian National Academy of Engineering, the Indian National Science Academy, The National Academy of Sciences, India, Allahabad, The Institution of Engineering and Technology, U.K., and The Institution of Electronics and Telecommunication Engineers, India, a life member of the Indian Society for Technical Education, and an associate member of The Institution of Engineers (India). He is an Area Editor for the IEEE TRANSACTIONS ON WIRELESS COMMUNICATIONS and an Editor for the IEEE TRANSACTIONS ON COMMUNICATIONS. He is a recipient of the Hari Om Ashram Prerit Dr. Vikram Sarabhai Research Award in the field of Electronics, Telematics, Informatics, and Automation, and of the Shanti Swarup Bhatnagar Prize in Engineering Sciences.

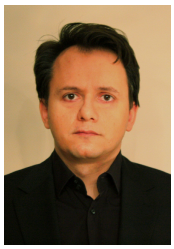

Nikos C. Sagias (S'03-M'05) was born in Athens, Greece in 1974. He received the BSc degree from the Department of Physics of the University of Athens, Greece in 1998. The MSc and PhD degrees in Telecommunication Engineering were both received from the same department, in 2000 and 2005, respectively. Since 2001, he has been involved in various National and European Research & Development projects for the Institute of Space Applications & Remote Sensing of the National Observatory of Athens, Greece. During 2006-2008, was a PostDoc Research Associate at the Institute of Informatics & Telecommunications of the National Centre for Scientific Research–"Demokritos," Athens, Greece. Currently, he is an Assistant Professor in the Department of Telecommunications Science & Technology of the University of Peloponnese, Tripoli, Greece.

Dr. Sagias research interests span the area of digital communications, and more specifically MIMO and cooperative diversity systems, fading channels, and statistical communications. In his record, he has over forty (40) papers in prestigious international journals and more than thirty (30) in the proceedings of world recognized conferences. He serves as an Editor for the IEEE TRANSACTIONS ON WIRELESS COMMUNICATIONS, while he has been a TPC member for various IEEE conferences (GLOBECOM'08, VTC'08F, VTC'09F, VTC'09S, etc). He is a co-recipient of the best paper award in the 3rd International Symposium on Communications, Control & Signal Processing (ISCCSP), Malta, March 2008. He is a member of the IEEE and IEEE Communications Society as well as the Hellenic Physicists Association.